Inorganic Chemistry

ARTICLE

pubs.acs.org/IC

Lanthanide-Mediated Supramolecular Cages and Host−Guest Interactions

Badr El Aroussi,[†] Laure Guénée,[‡] Prodipta Pal,[§] and Josef Hamacek*[,†]

[†]Department of Inorganic, Analytical and Applied Chemistry and [§]Department of Physical Chemistry, University of Geneva, 30 quai E. Ansermet, 1211 Geneva 4, Switzerland

[‡]Laboratory of X-ray Crystallography, University of Geneva, 24 quai E. Ansermet, 1211 Geneva 4, Switzerland

Supporting Information

ABSTRACT: The structure and thermodynamic properties of lanthanide complexes with a new tripodal ligand **L2** have been elucidated using different physicochemical methods. At stoichiometric ratios, the tetrahedral three-dimensional complexes with lanthanide cations are formed in acetonitrile with good stabilities. Despite minor structural changes comparing to previously investigated tripodal ligands, the resulting assembly exhibits different features revealed with the crystal structure of $[Eu_4\mathbf{L2}_4](OH)(ClO_4)_{11}$ (orthorhombic, *Pbcn*). Interestingly, the highly charged edifice contains an inner cage encapsulating a perchlorate anion. Such lanthanide mediated cage-like assemblies are rare, and may be of interest for different sensing applications. Indeed, the anionic guest can be exchanged with different anions. The related host−guest equilibria were investigated with NMR techniques. Various aspects of these reactions are qualitatively discussed.

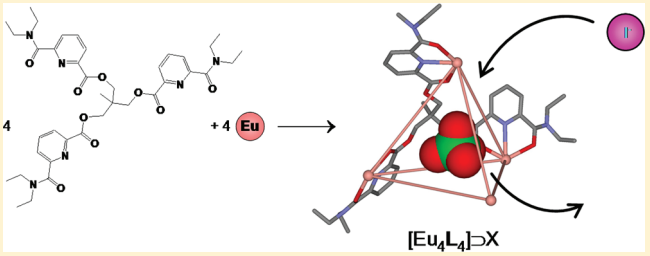

INTRODUCTION

Nowadays, supramolecular host−guest assemblies continue to inspire the scientific community for different reasons. In addition to aesthetically appealing structural aspects, the investigation of artificial systems contributes to a better understanding the nature, biological processes, and molecular recognition events. There are also a number of challenges connected with capturing or releasing compounds, modifying reactivity within container molecules (catalysis),[1] designing devices for energy conversion, separation sciences, and environmental applications, and so forth. The majority of receptors for cationic and anionic hosting is based on purely organic, often macrocyclic molecules, containing suitable interacting groups to stabilize a guest by weak supramolecular interactions between components.[2] However, metallo-organic architectures may also act as hosts for binding cations as well as anions.[3] In addition to the undeniable structural role, the incorporated metal ions may bring stronger and directional interactions with guests, or optional functionality.[4] Three-dimensional polynuclear assemblies represent an excellent potential for hosting and usually possess a cavity for accommodating different guests that may also act as a template for the edifice formation. A variety of supramolecular cages were reported by Fujita and co-workers.[5] Negatively charged supramolecular clusters $[M_4L_6]$ providing tetrahedral cages were extensively studied by Raymond and co-workers. Since the first report in 1998,[6] they have investigated various aspects of host−guest interactions including thermodynamics, dynamics, and catalysis.[7] Topologically similar hosting assemblies were used for neutral molecules[8,9] and a remarkable application stabilizing reactive phosphor was reported by Nitschke et al.[10] Similarly, anion-binding cages have been reported by different authors.[11,12] The above-mentioned metallo-organic hosts are built with main group and transition metal ions that ensure predictable stereochemical preferences for coordinating with bis-bidentate bridging ligands, and a good thermodynamic stability of self-assembled edifices. In this context, the formation of analogous lanthanide complexes having an internal cage is more problematic and there are only few examples employing lanthanide ions as building blocks.[13] In addition to a relative lability of their complexes, it is not trivial to design a suitable organic ligand (i) to satisfy high coordination numbers of Ln(III) and (ii) to achieve a good balance between flexibility and rigidity necessary for the self-assembly of polynuclear host receptors. However, we have recently succeeded to manage this challenging task in our laboratory. Connecting suitable coordinating units with an anchoring molecule (i.e., TAME) via an amide linker provides a tripodal ligand **L1** (Scheme 1).[14] The self-assembly of **L1** with Ln(III) cations leads to the formation of tetranuclear complexes with a tetrahedral arrangement of metallic cations that are complexed by helicoidally wrapped binding strands. In these edifices, the methyl group of the anchor points into the center of the tetrahedron (*endo*-CH_3), which limits the volume of the inner cavity that remains empty. Our present interest is thus focused on designing topologically similar organic receptors that allow to increase the cavity size for accommodating a guest molecule in the tetrahedral Ln(III) complexes.

Received: May 30, 2011
Published: July 28, 2011

Scheme 1. Structure of Tripodal Ligands L1 and L2

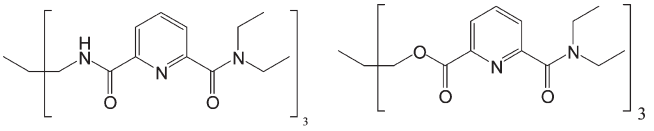

L1 L2

Scheme 2. Synthesis of the Tripodal Ligand L2

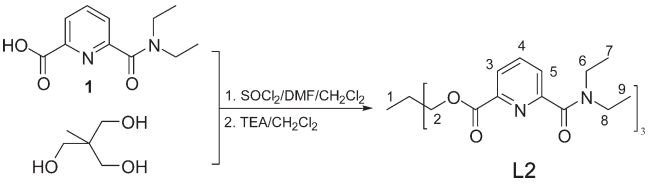

These recognition events may be potentially signaled with lanthanide luminescence and used for sensing applications.

In this work, we investigate Ln(III) complexes with a tripodal ligand **L2**, which is obtained by replacing the amide linker in **L1** with the ester functionality. The self-assembly processes with selected Ln(III) along the series are followed with different spectroscopic methods in solution. The formation of tetranuclear tetrahedral helicates with **L2** is confirmed with the crystal structure that reveals the encapsulation of a perchlorate anion inside the cage. Therefore, the host−guest exchange interactions of highly positively charged cages with anionic guests have been mainly investigated with NMR techniques using different nuclei (^{1}H, ^{19}F, ^{11}B, ^{35}Cl), which allows to identify the factors governing host−guest interactions within lanthanide-mediated supramolecular assemblies. The consequences of this minor structural modification will be discussed in relation with (i) the overall self-assembly process, and with (ii) physicochemical and luminescent properties.

RESULTS AND DISCUSSION

Synthesis of L2. The ligand was obtained by coupling of the carboxamidepyridine precursor **1** with a commercially available 1,1,1-trishydroxymethylethan according to the procedure described previously for **L1** (Scheme 2).[14a] The NMR spectrum of **L2** shows a set of nine well resolved peaks reflecting its C_3 symmetry. The signals were attributed with the COSY NMR technique.

Preparation and Characterization of Ln(III) Complexes with L2. The tetranuclear complexes were prepared by mixing of Ln(III) (Ln = La, Eu, Lu) with **L2** in equimolar ratios. The ESMS spectra of isolated compounds exclusively indicate the presence of tetranuclear complexes $[Ln_4\mathbf{L2}_4]^{12+}$ as a series of peaks belonging to perchlorate adducts. These associates are typically observed in analyses of highly charged polynuclear complexes, and a representative example is given for $[Eu_4\mathbf{L2}_4]^{12+}$ in Figure 1. The peaks observed for tetranuclear complexes with other Ln(III) are listed in Supporting Information, Table S1.

The ^{1}H NMR spectra of the tetranuclear complexes in acetonitrile (Ln = La, Eu, Lu) show only 12 signals related to one ligand strand, which is compatible with the formation of complexes with at least 3-fold rotation axis. The unambiguous attribution of signals was achieved with the two-dimensional NMR techniques (Supporting Information, Table S2). Moreover, the observation

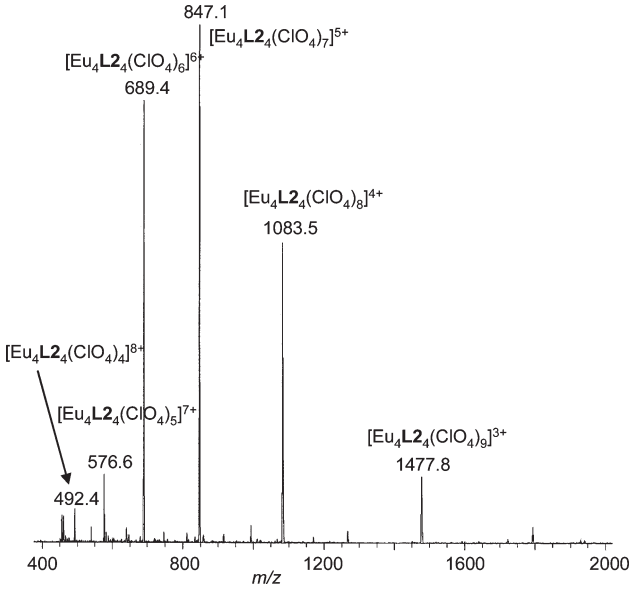

Figure 1. ESMS spectrum of $Eu_4\mathbf{L2}_4(ClO_4)_{12}$ in acetonitrile.

of diastereotopic protons H2−H2′, H6−H6′, and H8−H8′ is diagnostic for the Ln(III) complexation in a helical pattern. While the spectra with diamagnetic cations are reminiscent to those with **L1**, the spectrum measured for the Eu(III) complex (Figure 2) significantly differs from the spectrum of $[Eu_4\mathbf{L1}_4]^{12+}$. A closer inspection shows that the signal of the methyl proton H1 is not significantly influenced by the complexation in comparison with a strong shift $\delta_{H1}^{Eu_4\mathbf{L1}_4} \sim 13$ ppm in $[Eu_4\mathbf{L1}_4]^{12+}$. Moreover, the diastereotopic protons H2 and H2′ are strongly shifted downfield with the concomitant splitting $\delta_{H2}^{Eu_4\mathbf{L2}_4} \sim 5.5$ ppm, contrary to $\delta_{H2}^{Eu_4\mathbf{L1}_4} \sim 2$ ppm. Both observations indicate that the ligand **L2** self-assembles with Ln(III) cations in a different way, but the helical wrapping of binding strands is maintained. The ^{1}H NMR spectrum recorded in situ for the 1:1 reaction mixture with Ln(III) is identical to that recorded for the isolated solid complex $[Ln_4\mathbf{L2}_4](ClO_4)_{12}$ (Supporting Information, Figure S1).

Crystal Structure of $[Eu_4\mathbf{L2}_4](OH)(ClO_4)_{11}$. The X-ray quality crystals were obtained by recrystallization of the isolated complex from an acetonitrile/methanol solution. The crystal structure indeed confirms the composition and the tetrahedral scaffold of the complex $[Eu_4\mathbf{L2}_4]^{12+}$ determined with ESMS (Table 1, Figure 3 and Supporting Information, Figure S2). The complex is chiral, and the crystal is a racemate. The tetrahedral complex nearly possesses the rotation symmetry of the tetrahedron *T*, whereby the pseudo-3-fold axes pass through anchoring carbon atoms. These latter features are reminiscent to the complexes with **L1**. However, all anchoring methyl groups direct out of the tetrahedron center (*exo*-CH_3), contrary to $[Tb_4\mathbf{L1}_4]^{12+}$ (*endo*-CH_3).[b1] This configuration explains a moderate chemical shift observed for these protons with NMR. In addition to 1 OH^- anion and 10 noncoordinated perchlorates, 1 perchlorate anion is placed in the cage with oxygen atoms pointing toward Eu(III) cations. The average Eu···Eu distance is 10.73(1) Å, which is about 0.9 Å longer than in $[Tb_4\mathbf{L1}_4]^{12+}$.[14] Moreover, the average distance between the tetrahedron center and Eu(III) cations rises by 0.6 Å to 6.6(2) Å and clearly shows the expansion of the cavity. The bond lengths between coordinating atoms and europium cations are given in Supporting Information, Table S3. The coordination polyhedron can be best described as a distorted tricapped trigonal

dx.doi.org/10.1021/ic201156q |*Inorg. Chem.* 2011, 50, 8588–8597

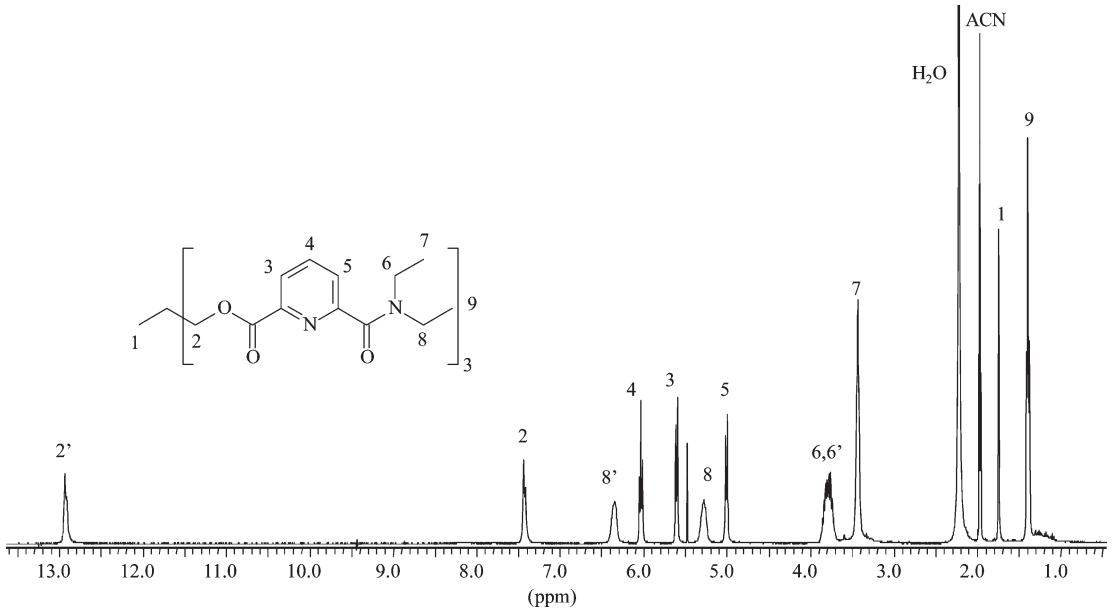

Figure 2. ^{1}H NMR spectrum of $[Eu_4\mathbf{L2}_4](ClO_4)_{12}$ in CD_3CN (293 K).

Table 1. Crystallographic Data for $[Eu_4\mathbf{L2}_4](OH)(ClO_4)_{11}$

chemical formula	$[Eu_4(C_{38}H_{48}N_6O_9)_4](OH)(ClO_4)_{11}.(H_2O)_7$		
formula weight	4761.09	D_x/gcm^{-3}	1.465
cryst. system	orthorhombic	V/Å^3	21587.6(18)
space group	*Pbcn*	μ/mm^{-1}	1.376
a / Å	25.1120(13)	refln collected	78′250
b / Å	37.4052(15)	independent refln	13787 (R_{int} = 0.096)
c / Å	22.9822(11)	R_1	0.1274
$\alpha = \beta = \gamma$ / deg	90	ωR_2	0.2360

prism. The distances between planes defined by coordinating atoms (Supporting Information, Figure S3) are equal to d(F1−F2) = 1.53(1) and d(F2−F3) = 1.81(3) Å. The average helical pitches about the complexed metal centers[15] are equal to 11.1(2) Å and 12.0(3) Å between planes F1−F2 and F2−F3, respectively. This slight relaxation of the helical twist and significantly longer distances Eu···O2 may be the consequences of the presence of ClO_4^- in the inner cavity. Interestingly, the diastereotopic proton H2′ is directed into the internal cavity and emerges relatively close to the oxygen atom of the perchlorate anion (d(H2···O) = 2.45 Å).

^{1}H NMR Titration. To establish the speciation of Ln(III) complexes in acetonitrile, ^{1}H NMR experiments were carried out with selected lanthanides ions (Ln = La, Nd, Eu, and Lu) by varying the [Ln]/[**L2**] ratio from 0 to 2 ([**L2**] ∼ 1.4 × 10^{-2} M). The spectra were recorded at least 1 h after the addition of Ln(III) solution to ensure sufficient equilibrating of the solutions. The evolution of ^{1}H NMR spectra is easy to follow. For titrations with all Ln(III), we observe a continuous decrease of the ligand signals with the metal addition. The peaks also become broader and less resolved, which indicates the presence of several exchanging species in equilibrium. These peaks disappear at about [Ln]/[**L2**] = 0.8−0.9. A further increase of Ln(III) concentration gives rise to new signals, whose maximum intensity is reached at [Ln]/[**L2**] ∼ 1. For the ratios [Ln]/[**L2**] > 1, two situations must be considered. First, in case of Nd(III), Eu(III), and Lu(III), the $[Ln_4\mathbf{L2}_4]^{12+}$ species is maintained in solution

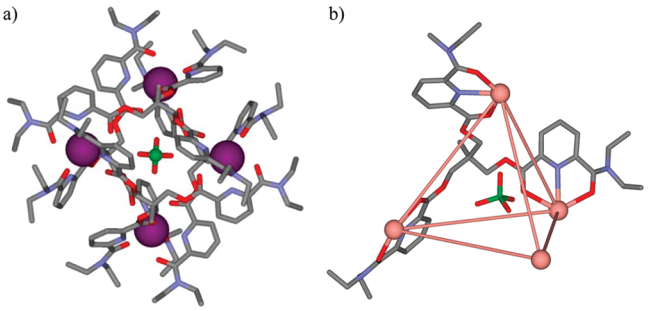

Figure 3. Molecular structure of $Eu_4\mathbf{L2}_4(ClO_4)_{12}$. (a) View of the whole complex. (b) Detailed view of the coordinated ligand within the tetrahedral structure. Hydrogen atoms, uncoordinated anions and solvent molecules are omitted for clarity.

until the end of the titration ([Ln]/[**L2**] ∼ 5 equiv) as the unique complex observed (Supporting Information, Figure S4). Second, the tetranuclear complex with La(III) undergoes a further transformation. Its concentration continuously decreases, and the signal vanishes at [La]/[**L2**] ∼ 1.5 (Figure 4 and Supporting Information, Figure S5). New signals simultaneously emerge, and the ^{1}H NMR spectrum at [La]/[**L2**] ∼ 1.5 (Figure 4) is consistent with the presence of a D_3-symmetrical complex $[La_3\mathbf{L2}_2]^{9+}$ with equivalent strands of both ligands. The trinuclear species $[Ln_3\mathbf{L1}_2]^{9+}$, where two strands belonging to two different ligands coordinate one metal ion, were already observed with analogous **L1**.[14b] Therefore, we suggest a similar coordination sphere in complexes with **L2**, whereby both ligands adopt the same conformation providing a triangular complex with an overall D_3 symmetry.

ESMS Titrations. Parallel ESMS titrations were performed for the mixtures of $Ln(ClO_4)_3 \cdot xH_2O$ (Ln = La, Eu, Lu) with **L2** ([**L2**] = 3 × 10^{-4} M) at different stoichiometries ([Ln]/[**L2**] = 0−2) in acetonitrile. At low Ln(III) concentration ([Ln]/[**L2**] ≤ 0.8), the signals of free **L2** are predominantly present, in addition to some species with 1:2, 1:3 stoichiometries, whose abundance is low (Supporting Information, Figure S6). For higher

dx.doi.org/10.1021/ic201156q |*Inorg. Chem.* 2011, 50, 8588–8597

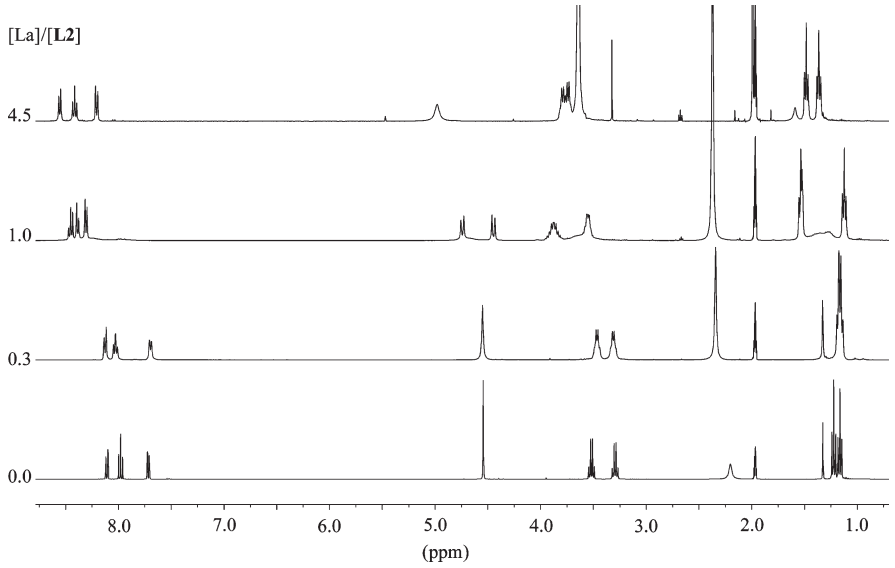

Figure 4. ^{1}H NMR titration of **L2** with lanthanum perchlorate (CD_3CN, 293 K).

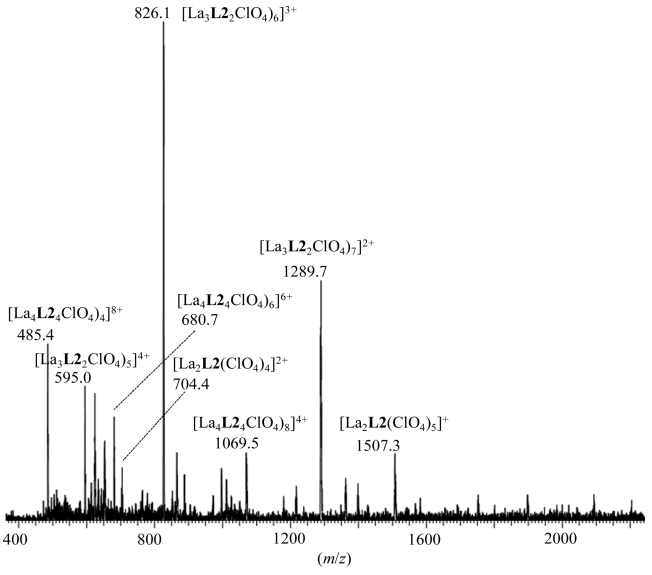

Figure 5. ESMS spectrum for [La]/[**L2**] = 2.

[Ln]/[**L2**] ratios, the detailed analysis of spectra and isotopic profiles of peaks shows two situations depending on the used lanthanide ion. For Ln = Eu and Lu, the $[Ln_4\mathbf{L2}_4]^{12+}$ species are exclusively detected even for the [Ln]/[**L2**] ratio higher than two. However, the titration with La(III) ion shows the formation of the $[La_4\mathbf{L2}_4]^{12+}$ only at about the 1:1 ratio. The ESMS spectrum recorded at [Ln]/[**L2**] ∼ 2 shows the series of peaks belonging to $[La_3\mathbf{L2}_2]^{9+}$ perchlorate adducts, which evidence the expected stoichiometry in excess of La(III) (Figure 5). The speciation measured with ESMS is thus in a good agreement with the data provided by ^{1}H NMR experiments.

Spectrophotometric Titrations. The stability constants of Ln(III) complexes with **L2** were determined in acetonitrile for Ln = La, Eu, and Lu by means of spectrophotometric titrations. The absorption spectra of **L2** in acetonitrile exhibit a large band centered about 267 nm and assigned to $n \rightarrow \pi^*$ and $\pi \rightarrow \pi^*$ transitions related to the pyridinedicarbonyl units.[14] Upon complexation with Ln(III), a bathochromic shift of the maximum to 279.5 nm with the concomitant appearance of a shoulder at ∼284 nm is observed (Supporting Information, Figure S7a). The absorption spectra were recorded for the [Ln]/[**L2**] ratio between 0 to 5 allowing the samples to equilibrate within 20 min after each addition of a metal ion solution. The factor analysis points out the presence of several absorbing species, whose formation constants β_{mn} are defined with equilibria eqs 1−3. While the changes of the absorption spectra are not obvious in excess of ligand, the inflection point at [Ln]/[**L2**] = 1 clearly indicates the formation of $[Ln_4\mathbf{L2}_4]^{12+}$ species for all lanthanides (Supporting Information, Figure S7b). The continuous evolution of spectra for the titration with La(III) ([La]/[**L2**] ratio >1) fits with the formation of $[La_3\mathbf{L2}_2]^{9+}$. Finally, the best fit with the SPECFIT software was obtained according to the equilibria eqs 1 and 2 for Ln = Eu, Lu and using equilibria 1−3 for La (Table 2). The fitted electronic spectra are given for Eu(III) and La(III) in Figure 6a and Supporting Information, Figure S8, respectively.

Table 2. Experimental Stability Constants for the Complexes with L2

Ln(III)	$1/r$ [Å^{-1}]	$\log \beta_{13}$	$\log \beta_{44}$	$\log \beta_{32}$
La	0.8197	17.2 ± 1.4	35.3 ± 1.5	19.0 ± 1.2
Eu	0.8929	13.6 ± 0.2	34.0 ± 0.3	
Lu	0.9709	15.6 ± 0.5	34.4 ± 0.6	

$$Ln(III) + 3\mathbf{L2} \rightleftarrows [Ln\mathbf{L2}_3]^{3+} \qquad \beta_{13} \qquad (1)$$

$$4Ln(III) + 4\mathbf{L2} \rightleftarrows [Ln_4\mathbf{L2}_4]^{12+} \qquad \beta_{44} \qquad (2)$$

$$3Ln(III) + 2\mathbf{L2} \rightleftarrows [Ln_3\mathbf{L2}_2]^{9+} \qquad \beta_{32} \qquad (3)$$

The stability constants of $[Ln\mathbf{L2}_3]^{3+}$ and $[Ln_4\mathbf{L2}_4]^{12+}$ do not significantly vary along the lanthanide series within experimental errors (Supporting Information, Figure S9).

dx.doi.org/10.1021/ic201156q |*Inorg. Chem.* 2011, 50, 8588–8597

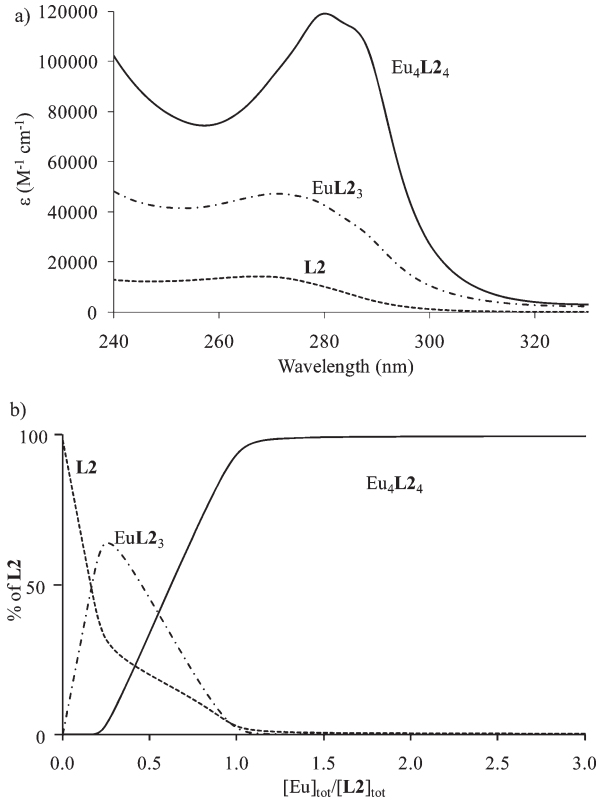

Figure 6. Spectrophotometric titration of **L2** with Eu(III). (a) Fitted absorption spectra of **L2**, $[EuL2_3]^{3+}$, and $[Eu_4L2_4]^{12+}$. (b) Distribution curves as the function of Eu(III) additions to **L2**. [**L2**] = 2×10^{-4} M.

While $\log \beta_{13}$ (Ln = Eu and Lu) and $\log \beta_{32}$ (Ln = La) are almost alike for **L1** and **L2**, $\log \beta_{44}$ calculated for $[Ln_4L2_4]^{12+}$ (Ln = Eu and Lu) are smaller than the values found for the carboxamide analogues $[Ln_4L1_4]^{12+}$ by approximately four units. This is obviously the consequence of a different structure of the assembly with **L2**, in addition to weaker interactions between Ln(III) and the ester groups. However, the self-assembly process with **L2** gives fewer complex species than **L1**. The established thermodynamic model and the observed overall speciation closely agrees with NMR and ESMS titrations. For Ln = Nd−Lu, the tetranuclear complex is exclusively formed over a wide range of metal/ligand ratios, which demonstrates its relative stability for potential applications (Figure 6b).

Photophysical Properties of $[Eu_4L2_4]^{12+}$. To alternatively prove the coordination mode of $[Eu_4L2_4]^{12+}$ and to evaluate the efficiency of the energy transfer between the ligand and Eu(III), the photophysical properties of this complex were studied in the solid state and in solution. The emission spectra show typical bands arising from Eu(III) excited levels, which are attributed to $^5D_0 \rightarrow {}^7F_j$ ($j = 0-6$) transitions. The excitation spectrum gives the evidence for the intersystem crossing (ISC) followed by the energy transfer from triplet states to the ^5D_j manifold of the lanthanide cation (Supporting Information, Figure S10a). The high-resolution emission spectrum at 10 K of $[Eu_4L2_4](ClO_4)_{12}$ in the solid state (Figure 7) is reminiscent to that of the analogous complex $[Eu_4L1_4](ClO_4)_{12}$ bearing the same coordinating atoms. The overall emission profile is thus compatible with a local pseudo-C_3 site symmetry. Moreover, a unique band for the symmetry sensitive transition Eu($^5D_0 \leftarrow {}^7F_0$) indicates the presence of only one crystallographic site for Eu(III) ions. The luminescence

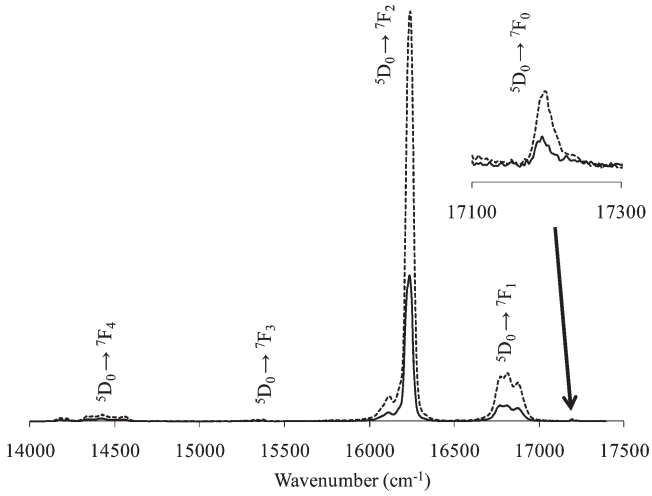

Figure 7. Metal-centered emission spectrum of $[Eu_4L2_4]^{12+}$ (solid state, 10 K, λ_{exc} = 308 (dashed lines) and 395 (solid lines) nm).

lifetime was measured by monitoring intense $^5D_0 \rightarrow {}^7F_2$ transitions and amounts to 1.59(1) ms. This lifetime falls in the range of values measured for similar compounds with completely saturated and well protected coordination sphere of Eu(III).[14] In acetonitrile, similar but low-resolved emission spectra were recorded upon the ligand-centered excitation at 279 nm (Supporting Information, Figure S10b). Interestingly, monoexponential fitting of the luminescence decay (λ_{em} = 616 nm) provides τ = 2.19(2) ms, which is longer than in the solid state. The determined quantum yield ($\Phi_{abs} = 7.8 \times 10^{-4}$) is slightly higher than that of $[Eu_4L1_4]^{12+}$ but does not attain the remarkable value measured for dipicolinate diethylester.[16] The ISC process remains poor and indicates an inadequate matching between the excited states of **L2** and those of the acceptor Eu(III).

Host−Guest Interactions of $[Eu_4L2_4]^{12+}$ Cage Complexes with Anions. As established with the X-ray crystal structure, the self-assembled complex $[Eu_4L2_4]^{12+}$ has an internal cavity with sufficient space for accommodating a perchlorate anion, which is stabilized inside by weak electrostatic interactions. Each oxygen atom of ClO_4^- is directed toward one positively charged Eu(III) cation in the vertex of the tetrahedron. The calculated volume of the cavity is around 91 Å that limits the size of the entering anion and contributes to selectivity. A perchlorate anion[17] occupies about 64% of the cage volume. That value falls to the upper limit for optimal encapsulation proposed by Mecozzi and Rebek,[18] but remains reasonable for a polar guest. The tetrahedral shape of the cavity seems to be better predisposed for tetrahedral anions matching this geometric preorganization. To unambiguously reveal the presence of these cage complexes also in solution, we have resorted to ^{35}Cl NMR measurements, which works well for inorganic systems.[19] Since the charge of isolated tetranuclear complexes is compensated with 12 perchlorate anions, we should measure two different signals for ClO_4^- in the ratio of intensities 11:1. Indeed, we observe two peaks separated by 10.6 ppm with the areas approximately in the expected ratio, which are related to free and encapsulated perchlorates, respectively (Figure 8a).

Since the guest binding occurs in solution, we were interested to examine host−guest interactions of different anions (X^{n-}) with the cage complexes with respect to their capacity to replace the perchlorate in the cage. The exchange reactions may be conveniently studied with NMR by monitoring the signals of

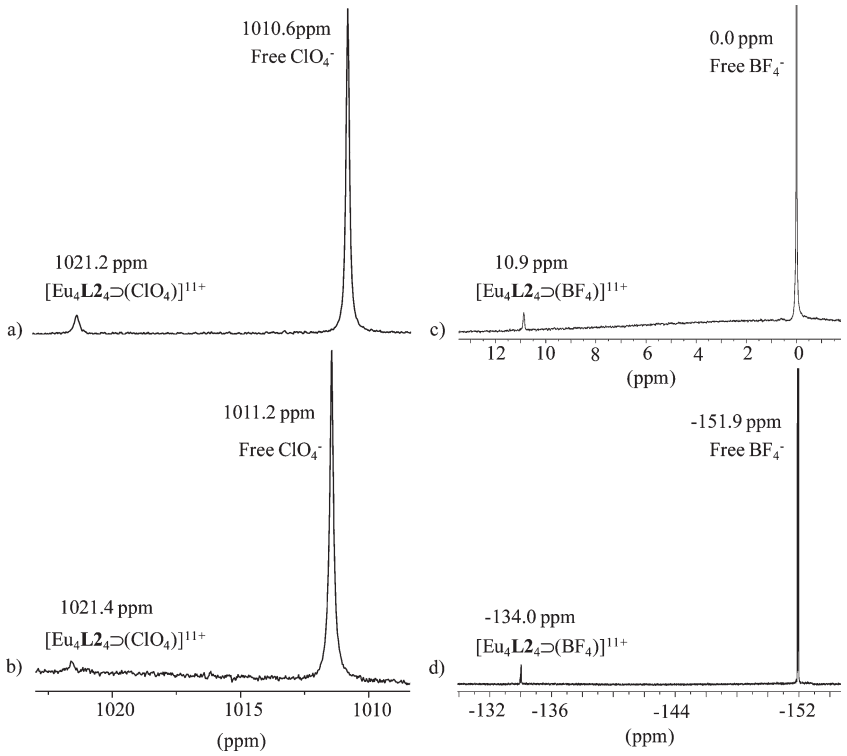

Figure 8. (a) ^{35}Cl NMR spectrum of $Eu_4\mathbf{L2}_4(ClO_4)_{12}$ in CD_3CN. The NMR spectra of the same solution after the addition of 12 equiv of BF_4^-: (b) ^{35}Cl, (c) ^{11}B, and (d) ^{19}F. The spectra were measured at room temperature.

different nuclei. In these studies, the europium complex $[Eu_4\mathbf{L2}_4](ClO_4)_{12}$ was used because of its weak paramagnetism resulting in the observation of well separated ^{1}H signals suitable for detecting minor structural changes within the complexes. The host−guest equilibria with several anions were followed by adding corresponding tetraalkylammonium salts to a solution of $[Eu_4\mathbf{L2}_4](ClO_4)_{12}$ in CD_3CN (equilibrium 4). The additions were done stepwise, up to 12 equiv of anions with respect to the tetranuclear complex accompanied with 12 perchlorate counterions. The samples were allowed to equilibrate at room temperature or at ∼40 °C for several hours.

$$\{[Eu_4\mathbf{L2}_4] \supset ClO_4^-\}^{11+} + X^{n-} \underset{k_{-1}}{\overset{k_1}{\rightleftharpoons}} \{[Eu_4\mathbf{L2}_4] \supset (X^{n-})\}^{(12-n)+} + ClO_4^- \qquad K_{eq} \tag{4}$$

The exchange reaction was first performed with a weakly coordinating BF_4^- anion structurally reminiscent of the tetrahedral ClO_4^-. With the addition of BF_4^-, a new set of signals appears in the ^{1}H NMR spectrum (Figure 9). These signals are closely related to the initial set except for different chemical shifts, which indicates the presence of the tetranuclear europium complex accommodating one BF_4^- anion inside the cavity. As expected, the difference is more pronounced for protons suffering from stronger paramagnetic effects (H2′, H2−H5). The exchange process is evidenced with the decrease of the signal corresponding to encapsulated perchlorates in the ^{35}Cl NMR spectrum (Figure 8b). Moreover, the presence of BF_4^- in the cavity is confirmed by ^{19}F NMR and ^{11}B experiments, whereby the observation of two different signals in the expected intensities is attributed to free and encapsulated BF_4^-, respectively (Figure 8 c,d). At equilibrium, the relative quantities of perchlorate- or tetrafluoroborate-containg cage complexes can be obtained by integrating related peaks in the ^{1}H NMR spectrum. After the addition of 12 equiv of BF_4^- ($[BF_4^-]_{tot} \cong [ClO_4^-]_{tot}$), we detect approximately 57% of $\{[Eu_4\mathbf{L2}_4]\supset(ClO_4^-)\}^{11+}$ and 43% of $\{[Eu_4\mathbf{L2}_4]\supset(BF_4^-)\}^{11+}$ in the reaction mixture. The related equilibrium constant K_{eq} (eq 4, $X^{n-} = BF_4^-$) is estimated to be about 0.7, taking into account a large excess of both anions.

The addition of more coordinating tetrahedral sulfate anions induces also the appearance of signals belonging to the tetranuclear complexes with encapsulated SO_4^{2-}. However, the signals of free **L2** appear because of the simultaneous destruction of a part of the tetranuclear complexes resulting from the sulfate complexation of Eu(III). Similar effects are observed for PO_4^{3-}, however, a bigger quantity of the complex is destroyed, in agreement with higher stability constants of lanthanide phosphates. Although both, SO_4^{2-} and PO_4^{3-}, clearly exhibit a good affinity for entering the tetrahedral cage, their tendency to directly complex lanthanide cations is greater. We have also examined the interactions of the cage complex with the series of halide anions, which have spherical shapes. Interestingly, the addition of I^- results in the complete exchange of ClO_4^- for I^- in the cage, which indicates much better affinity comparing with BF_4^- (K_{eq} ∼ 60). We observe also the formation of inclusion complexes with Br^-. However, a partial destruction of the host occurs and broad signals of **L2** are compatible with a slow exchange (on the NMR scale) between free **L2** and its unsaturated complexes. As expected, the affinity of halides for lanthanides is even stronger for Cl^- and F^-. While the exchanging ligand is revealed in the presence of Cl^- only at low temperature, the addition of F^- turns immediately to a complete extraction of Eu(III) from the complex,

dx.doi.org/10.1021/ic201156q |*Inorg. Chem.* 2011, 50, 8588–8597

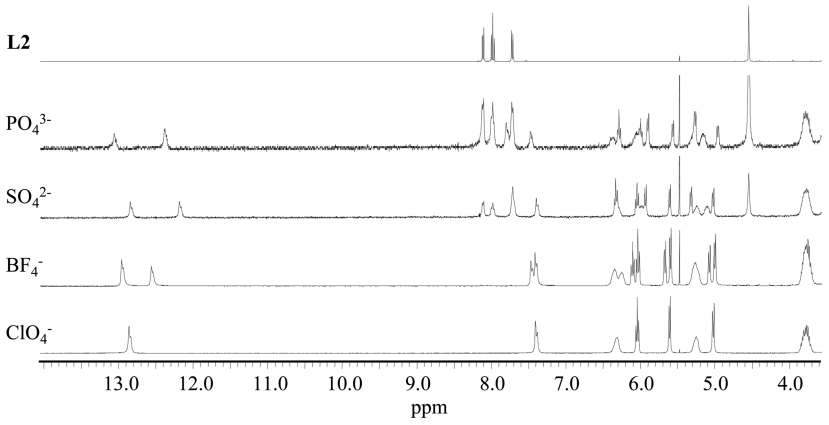

Figure 9. Changes of NMR spectra upon addition of tetrahedral anions (12 equiv BF_4^-, 2 equiv SO_4^{2-}, ~2 equiv PO_4^{3-}) to the CD_3CN solution of $\{[Eu_4\mathbf{L2}_4]\supset(ClO_4^-)\}^{11+}$.

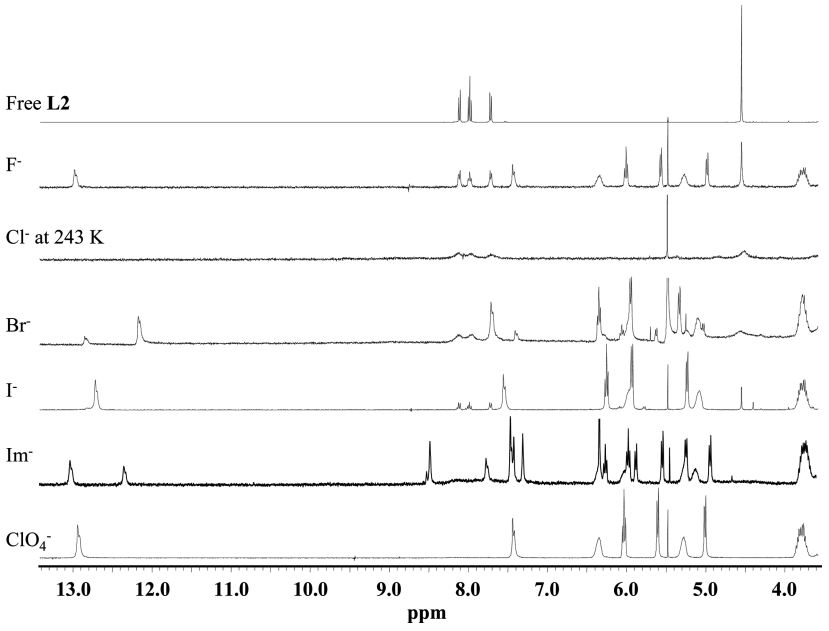

Figure 10. Changes of NMR spectra upon addition of monocharged anions (2 equiv F^-, 6 equiv Cl^-, 2 equiv Br^-, 12 equiv I^-, 6 equiv Im^-) to the CD_3CN solution of $\{[Eu_4\mathbf{L2}_4]\supset(ClO_4^-)\}^{11+}$.

and the spectrum shows only the signals of free **L2**. In addition to inorganic anions described above, we have examined possible interactions of the cage complex with imidazolate (Im^-), a small organic anion. As shown in Figure 10, the appearance of peaks belonging to a new complex evidence entering this anion in the cage ($K_{eq} \sim 1.6$). As well, the signals of encapsulated and free imidazolates are observed with no evidence for the destruction of the tetranuclear cage. The addition of pseudospherical PF_6^- anions into the solution of $\{[Eu_4\mathbf{L2}_4]\supset(ClO_4^-)\}^{11+}$ does not induce new signals in ^1H nor in ^{19}F NMR spectra, as predicted for its size being greater than the inner cavity.

Considering the above observations, we have attempted to qualitatively analyze host−guest interactions of the tetranuclear assembly with anions. First, some of the studied anions provoke the destruction of the complex, which is indicated by the ligand release. This behavior approximately reflects anion coordination affinities to Eu(III), which accordingly increase in the following series: $ClO_4^- \sim BF_4^- \sim Im^- < I^- < Br^- < Cl^- < SO_4^{2-} < PO_4^{3-} < F^-$. Interestingly, this sequence, with the exception of fluorides, matches the variation of anionic hydration free energies in Table 3 taken as a measure of electrostatic interactions. Second, the chemical shift difference of proton signals between $\{[Eu_4\mathbf{L2}_4]\supset(ClO_4^-)\}^{11+}$ and $\{[Eu_4\mathbf{L2}_4]\supset(X^{n-})\}^{(12-n)+}$ complexes ($\Delta\delta(Hi)$) was chosen as an indicator of structural and electronic perturbations induced by replacing ClO_4^- in the cage with another, in principle smaller anion (Table 3). Although all protons in the complex are affected with the anion exchange, $\Delta\delta(Hi)$ is the most sensitive for H2′ protons ($\delta \sim 13$ ppm), which are localized in a close proximity of encapsulated anions. The data in Table 3 shows that the examined anions, except BF_4^- and I^-, induce similar $\Delta\delta(Hi)$, which remains almost independent of anionic radius and charge, and consequently also hydration free energies. This effect may be tentatively attributed to their smaller sizes compared to that of ClO_4^- and thus a better fit

Table 3. Summary of Relevant Parameters for Selected Anions and Their Exchange Reactions with $\{[Eu_4L2_4]\supset(ClO_4)\}^{11+}$

X^{n-}	r_i (Å)[a]	Volume (Å^3)[e]	PC (%)[g]	ΔG_{hydr} (kJ/mol)[a]	$\Delta\delta$ (H2′)[h]	$\Delta\delta$ (H8)[h]	K_{eq}[i]
F^-	1.36	9.9	11	−465			
Cl^-	1.81[b]	24.8	27	−340			
Br^-	1.95[b]	31.5	35	−315	0.67	0.13	
I^-	2.16[b]	44.6	49	−275	0.14	0.15	60
ClO_4^-	2.36	57.9	64	−205	0	0	
BF_4^-	2.32	51.0	56	−190	0.39	0.04	0.7
SO_4^{2-}	2.30	51.0	56	−1080	0.66	0.13	
PO_4^{3-}	2.38	56.5	62	−2765	0.67	0.14	
PF_6^-	2.95[c]	105[f]					
Im^-	≤2.3[d]	≤51[f]	≤56		0.68	0.14	1.6

[a] Taken from ref 3c, p 6 and 225. [b] ref 20. [c] ref 21. [d] Estimated from the crystal structure in ref 22. [e] ref 17. [f] Calculated with r_i. [g] Packing coefficient PC = V_{anion}/V_{cage} (ref 18). [h] $\Delta\delta(Hi) = \Delta\delta_{X^{n-}}{}^{Hi} - \Delta\delta_{ClO_4^-}{}^{Hi}$. [i] Estimated from ^{1}H NMR spectra (measured at 273 K) with eq 4.

inside the cavity according to Rebek's rule (see packing coefficients in Table 3).[18] Since BF_4^- has almost the same size and shape as ClO_4^-, $\Delta\delta$ is relatively modest. In the case of spherical I^-, $\Delta\delta$ is even smaller and suggests similar positions of probing protons comparing with the ClO_4^- containing cage. In summary, the magnitude of $\Delta\delta(Hi)$ seems to be mainly influenced by steric interactions of anions reflecting their size and shape

The above host−guest equilibria can be also studied with ESMS. However, the formation of multicharged adducts of $\{[Eu_4L2_4]\supset(X^{n-})\}^{11+}$ with two kinds of anions, which may have different association affinities and instrumental responses, makes difficult an unambiguous identification of the cage complexes. Conclusive results can be possibly obtained when the exchange is complete, and we should observe the series of different anionic adducts with the cage containing one kind of encapsulated anions. In our case, these difficulties are illustrated for the exchange with I^-. The ESMS spectrum was recorded after adding 12 equiv of I^- to a solution of $[Eu_4L2_4](ClO_4)_{12}$, which led to the complete exchange confirmed with ^{1}H NMR. However, the detail in Supporting Information, Figure S11 shows the series of peaks corresponding to $[Eu_4L2_4(ClO_4^-)_n(I^-)_m]^{6+}$ $(n+m=6)$, which rather corresponds to a mixture of cage complexes with different anionic guests.

As mentioned previously, the exchange reactions with anions (eq 4) were carried out at 41(1)°C to attain the equilibrium more rapidly. To get the first insight into the exchange mechanism, the reaction kinetics were followed with ^{1}H NMR for the exchange with X^- = BF_4^- and I^-. Since both anions are in a large excess in relation to the cage complex ($[ClO_4^-]_{tot} \cong [X^-]_{tot}$), the variation of the peak area with time follows the kinetics of the pseudo-first order with $k_{obs} = (k_1 + k_{-1})[X^-]_{tot} = k'[X^-]_{tot}$. The fitted rate constants k' are thus estimated to be 4×10^{-4} M^{-1} s^{-1} and 1.1×10^{-3} M^{-1} s^{-1} for BF_4^- and I^-, respectively. The reaction with I^- is thus 2−3 times faster, and I^- obviously enters the cage more easily because of its spherical shape and smaller size. These low exchange rates depend on the anion nature, and we propose that anions pass in and out the cavity through structural apertures evidenced in the crystal structure.[7a] This suggestion is further supported by the fact that the rate of exchange is much slower than the complex dissociation induced by complexing anions such Br^- and SO_4^{2-}. At equilibrium, the exchange of free and encapsulated anions occurs in a slow exchange regime on the NMR time scale with no significant broadening of peaks (Figure 8). Moreover, variable temperature ^{11}B experiments show no coalescence of peaks related to encapsulated and free BF_4^- until 350 K. Despite the lability of Ln(III) complexes, the tetranuclear edifice remains stable, and the exchange reaction obviously does not require its partial dissociation, in concordance with the observations described for analogous supramolecular systems.[7a,9a,11b]

CONCLUSION

The present work reports on the preparation of new tetranuclear helicates built with lanthanide cations. The physicochemical characterization of complexes with selected Ln(III) (Ln = La, Nd, Eu, Lu) confirms the formation of tetrahedral $[Ln_4L2_4]^{12+}$ as the major species in solution for a wide range of [Ln]/[**L2**] ratios. These complexes are also thermodynamically stable in metal excess except $[La_4L2_4]^{12+}$, which transforms into the trinuclear complex $[La_3L2_2]^{9+}$. However, the major aspect of these tetranuclear assemblies stands in the formation of an inner cavity capable to accommodate an anion. This interesting feature arises because of an *exo*-CH_3 conformation adopted by **L2** that increases the cavity volume. The described behavior strongly contrasts with analogous $[Ln_4L1_4]^{12+}$ and illustrates that minor structural modifications in the ligand design may significantly influence the formation of a desired polynuclear assembly and its properties.

Taking advantage of these supramolecular assemblies, we have attempted to investigate host−guest interactions, mainly with NMR techniques. Indeed, a relatively large perchlorate anion initially localized in the cavity can be replaced with smaller anions. The existence of these equilibria has been meticulously demonstrated with tetrahedral, poorly coordinating anion BF_4^- by measuring ^{1}H, ^{35}Cl, ^{11}B, and ^{19}F spectra. Because of similar geometrical and chemical properties of ClO_4^- and BF_4^-, almost equimolar mixture of their cage complexes is observed at equilibrium. The exchange reaction truly occurs also with Im^- and I^-, and we could determine the equilibrium constants for these anions. However, at least partial breakdown of hosting $[Eu_4L2_4]^{12+}$ concomitantly takes place with other anions as the consequence of concurrent complexation reactions involving these anions and Ln(III). The chemical shift of H2′ protons chosen as a structural probe is independent of the charge and size of most anions, which may reflect their better sterical incorporation in the tetrahedral cavity comparing with $\{[Eu_4L2_4]\supset(ClO_4)\}^{11+}$. It is worth noting that the tetrahedral cage is capable of accommodating small organic anions, that is, imidazolate. On the contrary, the cavity size (91 Å^3) is not big enough for accommodating PF_6^-.

dx.doi.org/10.1021/ic201156q |*Inorg. Chem.* 2011, 50, 8588–8597

The exchange reactions proceed slowly, which suggests that the anion must squeeze into and out of the cavity rather than through the complex dissociation pathway.

The studied supramolecular system is a rare example of lanthanide-mediated polynuclear assembly capable of accommodating a guest molecule, and more particularly an anion. The exchange process is qualitatively observed for several anions despite some concurrent equilibria with few coordinating anions. The above-mentioned features can be further developed (i) in sensing systems using metal-centered luminescence and (ii) in catalytical procedures. These potential applications are currently investigated in our laboratory.

EXPERIMENTAL SECTION

Solvents and Starting Materials. These were purchased from Acros Organics, Fluka AG and Aldrich and used without further purification unless otherwise stated. *N*,*N*-dimethylformamide (DMF), acetonitrile, and dichloromethane were distilled over CaH_2. 6-(*N*,*N*-diethylcarbamoyl)pyridine-2-carboxylic acid (**1**) and monomethylester of dipicolinic acid (**2**) were prepared according to published procedures.[23] The perchlorate salts were prepared from the corresponding oxides (Rhodia and Aldrich, 99.99%) and dried according to published procedures. ***Caution!*** *Perchlorate salts are potentially explosive and should be handled carefully in small quantities.*[24] Ln(III) content of solid salts was determined by complexometric titrations with Titriplex III (Merck) in the presence of urotropine and xylene orange. Most of tetraalkylammonium salts of the different anions were purchased from suppliers, but the tetrabutylammonium salts of imidazolate, sulfate and phosphate were prepared in the laboratory by mixing of parent acids with an aqueous solution of $(Bu_4N)OH$. After stirring and evaporating the solvent, the obtained compounds were dried under vacuum. $(Bu_4N)Im$: Imidazole was added to a solution containing 1 equiv of $(Bu_4N)OH$. $(Bu_4N)_3(PO_4)$: A solution containing 3 equiv of $(Bu_4N)OH$ was added to a solution of H_3PO_4. Nevertheless, the presence of some monoprotonated HPO_4^{2-} can not be excluded. $(Bu_4N)_2(SO_4)$: $(Bu_4N)OH$ was added to aqueous H_2SO_4 until pH 7.

Synthesis of L2. 2-Carboxy-6-diethylcarboxamidepyridine (300 mg, 4.1 equiv) was activated with $SOCl_2$ (15 equiv) in CH_2Cl_2 at reflux for 1.5 h. The excess of $SOCl_2$ was evaporated, and the residue was dried under vacuum. After dissolving in CH_2Cl_2, the solution was added dropwise to the mixture of 1,1,1-tris(hydroxymethyl)ethane and triethylamine. The reaction was stopped after 12 h of refluxing. The solution was washed with water, and the organic solvent was evaporated on a rotary evaporator. The solid residue was purified on the chromatographic column (SiO_2, $MeOH/CH_2Cl_2$, 2−2.5% (v/v)). Finally, the isolated ligand **L2** was dried under vacuum (88% yield).

L2. ^{1}H NMR (CD_3CN, 22 °C): δ 1.14 (CH3, t, 3H), 1.20 (CH3, t, 3H), 1.30 (CH3, s, 1H), 3.27 (CH2, q, 2H), 3.49 (CH2, q, 2H), 4.52 (CH2, s, 2H), 7.69 (CH, d, 1H), 7.95 (CH, t, 1H), 8.08 (CH, d, 1H). ESI-MS (CH_2Cl_2): m/z 733.3 ($[\mathbf{L2}+H^+]^+$), 755.8 ($[\mathbf{L2}+Na^+]^+$), 771.7 ($[\mathbf{L2}+K^+]^+$).

Synthesis and Characterization of Ln(III) (Ln = La, Eu, Lu) Complexes. The tetranuclear complexes with selected Ln(III) were prepared analogously as described below for the Eu(III) complexes.

A 12.4 mg portion of **L2** is mixed with 1 equiv of $Eu(ClO_4)_3$ in propionitrile. Diffusion of *t*-butylmethyl-ether into this mixture provides a solid powder, which was isolated by filtration and dried under vacuum.

*[Eu$_4$**L2**$_4$](ClO$_4$)$_{12}$*. ^{1}H NMR (CD_3CN, 22 °C): δ 1.39 (CH3, t, 3H), 1.74 (CH3, s, 1H), 3.43 (CH3, t, 3H), 3.76 (CH2, m, 1H), 3.81 (CH2, m, 1H), 5.00 (CH, d, 1H), 5.27 (CH2, m, 1H), 5.60 (CH, d, 1H), 6.03 (CH, t, 1H), 6.35 (CH2, m, 1H), 7.42 (CH2, d, 1H), 12.92 (CH2, d, 1H). ESI-MS (CH_3CN): m/z 689.4 ($[Eu_4\mathbf{L2}_4(ClO_4)_6]^{6+}$). Elemental analysis of $[Eu_4\mathbf{L2}_4](ClO_4)_{12}.12H_2O$ (calc.): % C 36.87 (36.91), % H 4.13 (4.40), %N 6.73 (6.80).

*[La$_4$**L2**$_4$] (ClO$_4$)$_{12}$*. ^{1}H NMR (CD_3CN, 22 °C): δ 1.12 (CH3, t, 3H), 1.52 (CH3, s, 1H), 1.53 (CH3, t, 3H), 3.55 (CH2, m, 1H), 3.56 (CH2, m, 1H), 3.86 (CH2, m, 1H), 3.89 (CH2, m, 1H), 4.45 (CH2, d, 1H), 4.74 (CH2, d, 1H), 8.31 (CH, d, 1H), 8.38 (CH, d, 1H), 8.45 (CH, t, 1H). ESI-MS (CH_3CN): m/z 688.8 ($[La_4\mathbf{L2}_4(ClO_4)_6]^{6+}$).

*[Lu$_4$**L2**$_4$](ClO$_4$)$_{12}$*. ^{1}H NMR (CD_3CN, 22 °C): δ 0.92 (CH3, t, 3H), 1.51 (CH3, s, 1H), 1.54 (CH3, t, 3H), 3.31 (CH2, m, 1H), 3.48 (CH2, m, 1H), 3.93 (CH2, m, 1H), 3.95 (CH2, m, 1H), 4.37 (CH2, d, 1H), 4.73 (CH2, d, 1H), 8.25 (CH, d, 1H), 8.49 (CH, d, 1H), 8.54 (CH, t, 1H). ESI-MS (CH_3CN): m/z 704.9 ($[Lu_4\mathbf{L2}_4(ClO_4)_6]^{6+}$).

Spectroscopic and Analytical Measurements. NMR spectra were recorded on high-field NMR spectrometer (300 or 400 MHz, Bruker). NaCl in D_2O was used as the external reference for ^{35}Cl NMR.[25] Electronic spectra in the UV−vis were recorded from acetonitrile solutions with a Perkin-Elmer Lambda 900 spectrometer using quartz cells of 0.1 cm path length. Spectrophotometric titrations were performed with a J&M diode array spectrometer (Tidas series). The solutions of **L2** were titrated at 22 °C with a solution of $Ln(ClO_4)_3 \cdot xH_2O$ in acetonitrile, and after each addition the absorbance was recorded using Hellma optodes (optical path length 0.1 cm) immersed in the thermostatted titration vessel. Mathematical treatment of the spectrophotometric titrations was performed with the SPECFIT program.[26] Routine ESMS spectra were measured with a API 150EX LC/MS system. Pneumatically assisted electrospray (ESI-MS) mass spectra were recorded from 10^{-4} M acetonitrile solutions of Ln(III) complexes on a Finnigan SSQ7000 instrument with the optimized ionization temperature (150 °C) or on API III Applied Biosystem (ISV 3500 V/OR 30 V). Luminescence spectra and decays in solution were recorded on Perkin-Elmer LS-50B spectrometer. Emission and excitation spectra of solid samples were measured on a Horiba Fluorolog 3 instrument. The low temperature spectra were obtained using closed cycle cryostat (Janis-Sumitomo SHI-4.5). The luminescence lifetime was measured at room temperature, using the Spex 270 monochromator and SR 400 multi channel scalar. The Eu^{3+} was excited with 465 nm line of a CW Ar^+ laser which was chopped with mechanical chopper. The quantum yield of $[Eu_4\mathbf{L2}_4](ClO_4)_{12}$ in acetonitrile has been calculated according to the equation $\Phi x/\Phi_r = (A_r(\tilde{\nu})I_r(\tilde{\nu})n_x^2D_x)/(A_x(\tilde{\nu})I_x(\tilde{\nu})n_r^2D_r)$ where x refers to the sample and r to the reference (the solution of $[Eu(terpy)_3](ClO_4)_3$ in acetonitrile),[27] A is the absorbance, $\tilde{\nu}$ the excitation wavenumber used, I the intensity of the excitation light at this energy, n the refractive index, and D the integrated emitted intensity.

X-ray Crystal Measurements. The crystallographic data were collected at 150 K on a Stoe IPDS diffractometer with graphite monochromatic Mo[Kα] radiation (λ = 0.7107 Å). The structure was solved by direct methods (SIR97),[28] all other calculation were performed with SHELXL97.[29] Because of the large size of the unit cell, the crystal-image plate detector distance was increased to 90 mm, thus limiting the resolution to 2θ = 22.35°. Hydrogen atoms of disordered water and hydroxyl molecules were not included in the refined model. Twelve carbon atoms belonging to the terminal ethyl groups had highly anisotropic displacement parameters and were thus refined isotropically.

ASSOCIATED CONTENT

Supporting Information. Tables containing ESMS, NMR and crystallographic data, Figures with ^{1}H NMR spectroscopic data, ESMS spectra, spectrophotometric and luminescent data for the Ln(III) complexes with **L2**. A crystallographic CIF file for the structure of $[Eu_4\mathbf{L2}_4](ClO_4)_{11}(OH)$. This material is available free of charge via the Internet at http://pubs.acs.org.

AUTHOR INFORMATION

Corresponding Author
*E-mail: josef.hamacek@unige.ch.

ACKNOWLEDGMENT

Financial support from the University of Geneva and SNF is gratefully acknowledged. We thank P. Perrottet for recording the ESI-MS spectra, André Pinto for helping with NMR measurements of different nuclei, and H. Eder for performing the elemental analyses. We thank Prof A. Hauser and Dr. H. Hagemann for providing access to spectroscopy equipment.

REFERENCES

(1) (a) Breiner, B.; Clegg, J. K.; Nitschke, J. *Chem. Sci.* **2011**, *2*, 51–56. (b) Lützen, A. *ChemCatChem* **2010**, *2*, 1212–1214. (c) *Supramolecular catalysis*; van Leeuwen, P. W. N. M., Ed.; Wiley-VCH: Weinheim, Germany, 2008.

(2) Steed, J. W.; Atwood, J. L. *Supramolecular Chemistry*; John Wiley & Sons Ltd: Chichester, 2009.

(3) (a) Beer, P. D.; Hayes, E. J. *Coord. Chem. Rev.* **2003**, *240*, 167. (b) Rice, C. R. *Coord. Chem. Rev.* **2006**, *250*, 3190. (c) *Supramolecular chemistry of anions*; Bianchi, A., Bowman-James, K., García-España, E., Eds.; John Wiley & Sons, Inc.: New York, 1997.

(4) Beer, P. D.; Gale, P. A. *Angew. Chem., Int. Ed.* **2001**, *40*, 486.

(5) (a) Umemoto, K.; Yamaguchi, K.; Fujita, M. *J. Am. Chem. Soc.* **2000**, *122*, 7150–7151. (b) Fujita, M.; Tominaga, M.; Hori, A.; Therrien, B. *Acc. Chem. Res.* **2005**, *38*, 371–380.

(6) Caulder, D. L.; Powers, R. E.; Parac, T. N.; Raymond, K. N. *Angew. Chem., Int. Ed.* **1998**, *37*, 1840–1843.

(7) (a) Pluth, M. D.; Raymond, K. N. *Chem. Rev.* **2007**, *36*, 161–171. (b) Davis, A. V.; Raymond, K. N. *J. Am. Chem. Soc.* **2005**, *127*, 7912–7919. (c) Mugridge, J. S.; Bergman, R. G.; Raymond, K. N. *J. Am. Chem. Soc.* **2010**, *132* (4), 1182–1183. (d) Sgarlata, C.; Mugridge, J. S.; Pluth, M. D.; Tiedemann, B. E. F.; Zito, V.; Arena, G.; Raymond, K. N. *J. Am. Chem. Soc.* **2010**, *132*, 1005–1009. (e) Pluth, M. D.; Fiedler, D.; Mugridge, J. S.; Bergman, R. G.; Raymond, K. N. *Proc. Natl. Acad. Sci. U.S.A.* **2009**, *106* (10438−10443), S10438/1–S10438/62. (f) Pluth, M. D.; Bergman, R. G.; Raymond, K. N. *Acc. Chem. Res.* **2009**, *42*, 1650–1659. (g) Pluth, M. D.; Johnson, D. W.; Szigethy, G.; Davis, A. V.; Teat, S. J.; Oliver, A. G.; Bergman, R. G.; Raymond, K. N. *Inorg. Chem.* **2009**, *48* (1), 111–120. (h) Mugridge, J. S.; Berridge, R.; Raymond, K. N. *Angew. Chem., Int. Ed.* **2010**, *49* (21), 3635–3637.

(8) Liu, T.; Liu, Y.; Xuan, W.; Cui, Y. *Angew. Chem., Int. Ed.* **2010**, *49*, 4121–4124.

(9) (a) Mal, P.; Schultz, D.; Beyeh, K.; Rissanen, K.; Nitschke, J. R. *Angew. Chem., Int. Ed.* **2008**, *47*, 8297. (b) Riddell, I. A.; Smulders, M. M. J.; Clegg, J. K.; Nitschke, J. R. *Chem. Commun.* **2011**, *47*, 457.

(10) Mal, P.; Breiner, B.; Rissanen, K.; Nitschke, J. R. *Science* **2009**, *324*, 1697–1699.

(11) (a) Paul, R. L.; Bell, Z. R.; Jeffery, J. C.; McCleverty, J. A.; Ward, M. D. *Proc. Natl. Acad. Sci. U.S.A.* **2002**, *99* (8), 4883–4888. (b) Paul, R. L.; Argent, S. P.; Jeffery, J. C.; Harding, L. P.; Lynam, J. M.; Ward, M. D. *Dalton Trans.* **2004**, 3453–3458.

(12) Custelcean, R.; Bosano, J.; Bonnesen, P. V.; Kertesz, V.; Hay, B. P. *Angew. Chem., Int. Ed.* **2009**, *48*, 4025–4029.

(13) (a) He, C.; Lin, Z.; He, Z.; Duan, C.; Xu, C.; Wang, Z.; Yan, C. *Angew. Chem., Int. Ed.* **2008**, *47*, 877–881. (b) Liu, Y.; Wu, X.; He, C.; Jiao, Y.; Duan, C. *Chem. Commun.* **2009**, 7554–7556.

(14) (a) Hamacek, J.; Bernardinelli, G.; Filinchuk, Y. *Eur. J. Inorg. Chem.* **2008**, 3419–3422. (b) Hamacek, J.; Besnard, C.; Penhouet, T.; Morgantini, P.-Y. *Chem.—Eur. J.* **2011**, *17*, 6753–6764.

(15) Renaud, F.; Piguet, C.; Bernardinelli, G.; Bunzli, J.-C.; Hopfgartner, G. *J. Am. Chem. Soc.* **1999**, *121* (41), 9326–9342.

(16) Renaud, F.; Piguet, C.; Bernardinelli, G.; Bunzli, J.-C.; Hopfgartner, G. *Chem.—Eur. J.* **1997**, *3*, 1660–1667.

(17) Marcus, Y.; Jenkins, H. D. B.; Glasser, L. *Dalton Trans.* **2002**, 3795.

(18) Mecozzi, S.; Rebek, J., Jr. *Chem.—Eur. J.* **1998**, *4* (6), 1016–1022.

(19) (a) Tarasov, V.; Guerman, K.; Simonoff, G.; Kirakosyan, G.; Simonoff, M. *Proceedings of the NRC5: 5th International Conference on Nuclear and Radiochemistry*, Pontresina, Switzerland, September 3−8, 2002; Vol 2, pp 641−644. (b) Prakash, G. K. S.; Keyaniyan, S.; Aniszfeld, R.; Heiliger, L.; Olah, G. A.; Stevens, R. C.; Choi, H.-K.; Bau, R. *J. Am. Chem. Soc.* **1987**, *109*, 5123–5126.

(20) Park, C. H.; Simmons, H. E. *J. Am. Chem. Soc.* **1968**, 2431–2432.

(21) Robinson, R. A.; Stokes, J. M.; Stokes, R. H. *J. Phys. Chem.* **1961**, *65*, 542.

(22) Zurawski, A.; Mai, M.; Baumann, D.; Feldmann, C.; Muller-Buschbaum, K. *Chem. Commun.* **2011**, *47*, 496–498.

(23) Dalla Favera, N.; Guenee, L.; Bernardinelli, G.; Piguet, C. *Dalton Trans.* **2009**, 7625–7638.

(24) Raymond, K. N. *Chem. Eng. News* **1983**, *61*, 4.

(25) Harris, R. K.; Becker, E. D.; Cabral De Menezes, S. M.; Goodfellow, R.; Granger, P. *Pure Appl. Chem.* **2001**, *73*, 1795–1818.

(26) Gampp, H.; Maeder, M.; Meyer, C. J.; Zuberbuehler, A. D. *Talanta* **1986**, *33*, 943.

(27) Petoud, S.; Bunzli, J.-C. G.; Glanzman, T.; Piguet, C.; Xiang, Q.; Thummel, R. P. *J. Lumin.* **1999**, *82*, 69–79.

(28) Altomare, A.; Burla, M. C.; Camalli, M.; Cascarano, G.; Giacovazzo, C.; Guagliardi, A.; Moliterni, A. G. G.; Polidori, G.; Spagna, R. *J. Appl. Crystallogr.* **1999**, *32*, 115.

(29) Sheldrick, G. M. *SHELXL97 Program for the Solution and Refinement of Crystal Structures*; University of Göttingen: Göttingen, Germany, 1997.